AD-A115 927   CALIFORNIA UNIV BERKELEY DEPT OF CHEMICAL ENGINEERING   F/G 11/9
TRANSIENT STRUCTURES AND RHEOLOGICAL PROPERTIES OF SBS BLOCK CO--ETC(U)
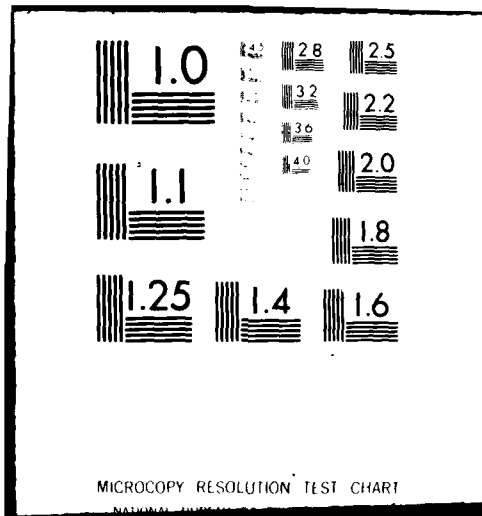JUN 82   N SIVASHINSKY, T J MOON, D S SOONG   N00014-81-K-0516
UNCLASSIFIED   TR-2   NL

END
DATE
FILMED
7-82
DTIC

MICROCOPY RESOLUTION TEST CHART
NATIONAL BUREAU

OFFICE OF NAVAL RESEARCH

Contract N00014-81-K-0516

TECHNICAL REPORT NO. 2

Transient Structures and Rheological Properties

of SBS Block Copolymer Melts

by

Naomi Sivashinsky, Tak Jin Moon and David S. Soong

Prepared for Publication

in the

Journal of Macromolecular Science - Physics

Department of Chemical Engineering,
University of California, Berkeley,
Berkeley, Ca. 94720

June 8, 1982

REPORT DOCUMENTATION PAGE		READ INSTRUCTIONS BEFORE COMPLETING FORM
1. REPORT NUMBER Technical Report No. 2	2. GOVT ACCESSION NO. AD-A115 927	3. RECIPIENT'S CATALOG NUMBER
4. TITLE (and Subtitle) Transient Structures and Rheological Properties of SBS Block Copolymer Melts		5. TYPE OF REPORT & PERIOD COVERED Technical Report May 1, 1981 - present
		6. PERFORMING ORG. REPORT NUMBER
7. AUTHOR(s) Naomi Sivashinsky, Tak Jin Moon and David S. Soong		8. CONTRACT OR GRANT NUMBER(s) N00014-81-K-0516
9. PERFORMING ORGANIZATION NAME AND ADDRESS Department of Chemical Engineering University of California at Berkeley Berkeley, Ca. 94720		10. PROGRAM ELEMENT, PROJECT, TASK AREA & WORK UNIT NUMBERS
11. CONTROLLING OFFICE NAME AND ADDRESS Office of Naval Research Arlington, VA 22217		12. REPORT DATE June 8, 1982
		13. NUMBER OF PAGES
14. MONITORING AGENCY NAME & ADDRESS(if different from Controlling Office)		15. SECURITY CLASS. (of this report) Unclassified
		15a. DECLASSIFICATION/DOWNGRADING SCHEDULE

16. DISTRIBUTION STATEMENT (of this Report)

This document has been approved for public release and sale; its distribution is unlimited

17. DISTRIBUTION STATEMENT (of the abstract entered in Block 20, if different from Report)

18. SUPPLEMENTARY NOTES

19. KEY WORDS (Continue on reverse side if necessary and identify by block number)

Morphology, Time-Dependent Properties, Block Copolymer, Elastic Recoil

20. ABSTRACT (Continue on reverse side if necessary and identify by block number)

Shear stress growth and relaxation behavior of two well-characterized SBS block copolymers has been studied using a Melt Elasticity Tester. Effects of casting solvents on the transient rheological properties and structure variation during flow are determined via samples cast from THF/MEK and cyclohexane. The temperature dependence of the observed shear stress at the yield point and steady-state viscosities provides insight into the mechanism of structure breakdown induced by the applied flow. Shear stress relaxation upon cessation of flow reveals complex behavior, depending on temperature, casting solvents

DD FORM 1473 EDITION OF 1 NOV 65 IS OBSOLETE
1 JAN 73

S N 0102-LF-014-6601

and duration of previous flow. Strain recovery data have also been obtained, indicating strong dependence on the composition of the copolymers. Significance of these observations in terms of the melt structure of SBS is discussed.

ABSTRACT

Shear stress growth and relaxation behavior of two well-characterized SBS block copolymers has been studied using a Melt Elasticity Tester. Effects of casting solvents on the transient rheological properties and structure variation during flow are determined via samples cast from THF/MEK and cyclohexane. The temperature dependence of the observed shear stress at the yield point and steady-state viscosities provides insight into the mechanism of structure breakdown induced by the applied flow. Shear stress relaxation upon cessation of flow reveals complex behavior, depending on temperature, casting solvents and duration of previous flow. Strain recovery data have also been obtained, indicating strong dependence on the composition of the copolymers. Significance of these observations in terms of the melt structure of SBS is discussed.

DTIC
COPY
INSPECTED
2

INTRODUCTION

Block copolymers often exhibit the phenomenon of microphase separation as a consequence of thermodynamic incompatibilities of the component blocks (1,2). This phase separation sometimes persists well into the molten state, giving rise to various complex rheological properties (3). For example, melt viscosities of SBS in certain temperature ranges were found to be higher than both a random copolymer (SBR) of comparable composition and molecular weight and either constituent homopolymer of the same molecular weight (4,6). This observation strongly suggested the multiphase nature of SBS in the liquid state. Small-amplitude oscillatory experiments resulted in dynamic viscosities, $\eta'(\omega)$, which lacked low-ω asymptotes, η_0, commonly associated with homogeneous fluids (3,6,7). Similarly, steady shear viscosities, $\eta(\dot{\gamma})$, at low $\dot{\gamma}$ did not tend to approach a Newtonian limit, η_0 (3,4,8). In addition, the measured viscosities were difficult to reproduce, as both the shear histories and duration of the rest period in between successive runs affected the experimental results to a large extent.

The aforementioned anomalies associated with SBS triblock copolymers were consistent with the existence of microphase-separated morphologies in the melt. When the fluid at rest was sheared, its multiphase structure began to degrade as the PS blocks were forced out of their domains to intermix with the PB matrix.' The response of the fluid at low $\dot{\gamma}$ or ω was reminiscent of a three-dimensional network of which the crosslinks were formed by the PS domains. At high PS contents, the domains might even coalesce to form a phase-separated structure with co-continuous phases. It was this sort of structure which endowed the fluid with distinct solid-like properties. The lack of low-ω or low-$\dot{\gamma}$ limits of the viscosities also suggested that a certain yield stress must be exceeded before molecular flow could commence.

This yield stress was required to initiate breakdown of the multiphase structure of the fluid (9,10).

Stress relaxation following cessation of steady shear for a long time failed to relieve the stress completely (3). Residual stress remained after the flow had stopped for a long time. Its magnitude was independent of $\dot{\gamma}$ over a wide $\dot{\gamma}$ range, but increased with the duration of the shear flow. The inability of the stress sustained by the fluid to relax completely was indicative either of the retention of some sort of microstructure at steady flow or the rapid recovery of phase-separated structure before the stress had the opportunity to decay to zero. Indeed, domains were found through electonmicroscopy in quenched samples which were subjected to shear rates as high as $10 \ sec^{-1}$ (3). The above solid-like characteristics disappeared when the system temperature exceeded a certain critical microphase separation temperature (8,11-13), whereupon the melt transformed into a homogeneous liquid. This again constituted strong evidence that the rheology of SBS triblock copolymers was highly sensitive to the prevailing morphology.

Casting solvents were shown to exert significant effects on the sample morphology (14-19). Selective solvation of one block caused that portion of the chains to expand in solution, but left the other block in a relatively collapsed state. The continuity of the block preferentially dissolved was thus promoted and could lead to the development of a three-dimensional network even when it was the minor component. Casting solvents thus played an important role in determining the rheological properties of SBS samples (14-19).

The above discussions revealed several complex rheological features associated with the SBS systems. The enhanced viscosity at low $\dot{\gamma}$ in steady flow, the existence of yield stress, and the lack of η_o could all be

explained in the light of fluid structure in the melt state. However, the evolution of the structure during flow and its recovery after flow have not yet been systematically investigated. In this work, the effects of casting solvent, temperature, and shear history upon the time-dependent stress growth and relaxation behavior are studied using a concentric-cylinder rheometer. Strain recovery data are also obtained with this device. Experimental results will be discussed to provide insight into the molecular processes of structure breakdown and reformation in SBS melts.

EXPERIMENTAL

1. Test Apparatus

A Melt Elasticity Tester (20) was used in this study to obtain stress growth and relaxation curves. Figure 1 gives the schematic drawings of the apparatus. This device employs a concentric cylinder geometry. The test fluid was kept between the inner cylinder and the outer cup, whose diameters are 0.476 cm and 0.637 cm. respectively. The curvature of the rheometer can be neglected in analyzing the data in view of the small gap size compared to the dimensions of the cylinders (20). A drive motor applies steady rotational motion to the outer cylinder. Several fixed angular speads are available, corresponding to a strain rate range from 0.66 sec^{-1} to 33.33 sec^{-1}. The cylinders are placed in a controlled-temperature chamber. A restraining arm attached to the inner cylinder is linked to a force transducer for stress measurement. The outer cylinder has a protrusion which hits the stop around the periphery of the rheometer to terminate the flow. Five additional locations have been chosen for placing the stop besides the original one provided by the instrument, so that the flow can be terminated at various total strains. The operating range after this modification now covers total deformations from 0.5 to 16 strain units. Output signals from the stress transducer were fed into a Linear fast-response strip-chart recorder with an average pen speed of 75 cm/sec, operating across a 25-cm wide chart paper.

When strain recovery data are desired, the load transducer is detached automatically from the restraining arm as soon as the protrusion hits the stop, allowing free rotation of the inner cylinder. The detachment is achieved through a solenoid device, which upon activation by the protrusion hitting the stop causes the tip of the transducer to retract rapidly. Light chopped at predetermined frequency travels through the optical fiber mounted

inside the light guide, leaving a series of images on the film in the camera. The developed film is subsequently analyzed to determine the location of the light dots, from which the strain recovery data are deduced.

2. Materials

The SBS samples used in this study were provided by the Shell Development Company. These are designated as TR-41-1648 and TR-41-1649. Table 1 lists some important molecular specifications and structural information.

Each polymer was dissolved in two solvents, cyclohexane and a mixed solvent of tetrahydrofuran (THF)/methylethylketone (MEK) (at a 90:10 volume ratio) to a concentration of about 10% by weight. These solutions were filtered to remove solid contaminants. Samples were prepared by spin casting from the solutions; the polymer films were dried at 60°C under vacuum until it reached a constant weight and then annealed at 110°C for one hour. The entire drying process usually required approximately two weeks.

3. Testing Procedure

Approximately 0.4g of the specimen was loaded into the outer cup at the beginning of each run. The cup was pre-heated to 154°C for TR-41-1649 and 180°C for TR-41-1648, whereupon the sample was introduced and kept in the cup for a few minutes until it softened sufficiently for insertion of the inner cylinder. The specimen was then allowed to reach thermal equilibrium at the desired test temperature before the experiment. The shear rates used throughout this study was 0.66 sec^{-1}. A fresh sample was used for each experiment.

RESULTS AND DISCUSSION

Stress transients following a sudden imposition of shear flow at $\dot{\gamma} = 0.66$ sec^{-1} for TR-41-1649 are shown in Figure 2. Note that all stress curves exhibit a pronounced maximum corresponding to the yield point. Prior to this yield point the stress rises rapidly, beyond which it decays slowly to eventually approach the steady-state level. The decay is particularly slow at the lower temperature, 119°C. Even at a total strain of 16 units, the stress has not levelled off. Differences between specimens prepared from THF/MEK and cyclohexane are discernible; the former constantly gives a slightly higher stress. Also shown in this figure is the stress curve obtained at 119°C for the sample cast from THF/MEK, but left in the Melt Elasticity Tester at 150°C for seven hours prior to testing. The result differs significantly from those of samples that have not been subjected to the long thermal exposure. The difference in the rheological properties could be rationalized in terms of heat-induced morphological rearrangement in the samples. However, the sample acquired a yellow tint after being at 150°C for seven hours, suggesting oxidative degradation which rigidified the material. A nitrogen purge was thus introduced during experimentation and a new sample was used for each run. Figure 3 shows the corresponding stress growth behavior for TR-41-1648. Similar to TR-41-1649, the stress increases with decreasing temperature. However, the difference between 119°C and 130°C is not as large as that exhibited by TR-41-1649. At 141°C the stress level is consistently higher than the corresponding TR-41-1649 data, although the overshoot peak has disappeared. Here, casting solvent also exerts a slight influence on the stress curves.

TR-41-1649 contains 48.2% PS by weight, in contrast to TR-41-1648 which has only 29.3% PS. The PS phase of the former may form a continuous network,

while the latter most likely have only isolated PS domains acting as physical crosslinks. Even if the domains indeed have enough connectivity, there may exist many weak points in the network. The integrity of the network would in principle dictate the stress level necessary to induce structure breakdown (thus yielding) if the structure was destroyed via fragmentation of the PS network at the weakest spots. This was apparently not the dominant process as TR-41-1648 exhibited higher yield values than TR-41-1649, contrary to predictions of the above mechanism. The other alternative to initiate structure breakdown is by pulling out individual PS blocks from their domains. This is expected to be the dominant process at high temperatures, according to a previous study on SBS solids (21).

The physical processes taking place in an SBS triblock copolymer melt under large deformations are thus assumed to be composed of several events in sequence. At low strains the deformation is largely sustained by stretching the elastomeric blocks of the molecules. If the stress is relieved, most of the strain can be recovered and the sample has not suffered plastic yielding. When the stress level builds up to the critical yield point, a substantial number of individual PS blocks which so far are anchored in the PS phase begin to be pulled out. In this block dislocation process, a particular segment along the PS block migrates from a PS-predominant environment through the interface (22-25) and eventually ends up in the PB matrix. Several barriers must be overcome to accomplish chain mingling. First, both PS and PB phases impart viscous resistance to flow. However, concerted movement of the various parts of the chain may not be necessary for flow, as the PB blocks are presumably already under much tension. In addition, the viscosity of the PS region is much greater than that operating in the PB phase. One can then ignore the viscous contribution of the PB phase to the observed yield

stress. If the yield stress indeed originated primarily from the frictional drag in the PS phase, its temperature dependence would correlate with predictions of the WLF equation for the viscosities of PS (26,27). The reference temperature in this equation is taken to be the glass transition temperature, T_g, which according to the Fox-Flory equation (28) is around 90°C for the PS blocks in our sample. This value is consistent with the occurrence of the damping peaks observed in dynamic mechanical measurements (21,23). Substitution of this reference temperature into the WLF equation gives a yield stress ratio on the order of 20 for the test temperatures of 119°C and 130°C. This is vastly different from the experimental ratios of 1.4 and 2.4 for TR-41-1468 and TR-41-1469, respectively, suggesting that a different mechanism must dominate the observed yield stress.

As the PS segment travels from its own environment to a chemically dissimilar PB surrounding, its chemical potential is elevated due to the thermodynamic incompatibility of the blocks. The chemical potential increase accompanying mixing of the blocks creates a "thermodynamic force barrier" (10), which further hinders molecular flow. If we assume that this additional energy requirement accounts for the major portion of the observed yield stress, the use of an Arrhenius relationship gives an activation energy of 9.2 Kcal/mole and 27 Kcal/mole for TR-16-1468 and TR-16-1469. These estimates are crude at best, however, they differ significantly from those for pure polystyrenes and polybutadienes (4). Note that TR-16-1468 has a much lower

activation energy than TR-16-1469. This is probably due to the weaker interconnectivity of the PS phase in the TR-16-1468 than TR-16-1469. The higher overall molecular weight of TR-16-1468, with its long PB middle block capable of forming entanglements, resulted in comparable levels of the observed steady-state stress at the test temperatures.

The slow downward turn of the shear stress beyond the yield point indicates that block pull-out occurs over a long period of time, and even at steady flow the chains may not be fully intermixed. Small aggregates of different sizes may flow as separate entities. As a result of the constant diffusive Brownian motion and the fact that these aggregates slide by one another as they are carried along by the shear motion, dislocated PS blocks may rejoin blocks in other aggregates. It is, however, difficult to predict the degree of these transient interconnections in the flowing fluid. As the structure gradually degrades, both the domain characters and the interphase profiles vary with time. The energy barrier required to pull out additional blocks may be appreciably lower than that needed to initiate the network disruption. At long times, the stress the fluid experiences is reduced to the steady-state level and further structural variation is substantially decreased. This does not preclude subtle changes in the average state of dynamic interactions among the aggregates over a long period, as the stress relaxation behavior discussed below reveals detectable differences following different durations of flow.

Stress relaxation upon cessation of flow for the two copolymers cast from THF/MEK is shown in Figures 4 and 5. TR-41-1649 in general exhibits a more rapid stress relaxation than TR-41-1648, although the steady-state viscosities are comparable. This suggests that the structure at steady flow and after cessation of flow is quite different between the two samples. Note also the significant difference in the rates of stress decay between the two test temperatures for TR-41-1649 and those for TR-41-1648. Temperature therefore plays a much more important role in the rheology of TR-41-1649 than TR-41-1648. This is consistent with the trend of temperature dependence observed in the corresponding stress growth experiment.

Effects of casting solvent on the stress relaxation behavior are shown in Figures 6 and 7. THF/MEK cast samples relax at a slower rate than samples prepared from cyclohexane solutions. The difference might have been even greater, had the samples not been subjected to the brief heating period required for loading into the test device.

As noted previously, the fluid structure upon flow degrades gradually. Therefore, if the flow is suddenly stopped after the fluid has been sheared for different durations, the fluid will have reached different structural states. Since subsequent stress relaxation is dictated by this structure, its behavior reveals important information about the structure degradation process. Stress relaxation curves, $\sigma(t)$, normalized by the initial stress level, σ_o, when the flow has just stopped for the two SBS samples sheared to different extents, are shown in Figures 8 and 9. Position 2 corresponds to a total strain of 1.1 strain units which is prior to the yield point, whereas position 4 occurs at a total strain of 3.2 strain units which lies on the downward side of the stress peak before steady state is attained. Stress relaxation is slower when the flow is terminated before the yield point is reached, i.e., before the original fluid structure is substantially altered. Difference in the rate of stress relaxation following shear of varying durations appears to be more distinct for TR-41-1648, suggesting that this sample undergoes a larger overall structure change during shear. In this context, disentanglement of the PB blocks may play a major role in TR-41-1648.

Note that in the above stress relaxation curves, the logarithm of the normalized stess, σ/σ_o, is plotted versus time. It is clear that one single relaxation time, λ, cannot describe the entire stress relaxation behavior of such morphologically and rheologically complex systems. Otherwise, the above

semi-log plots would give straight lines as dictated by $\ln \frac{\sigma(t)}{\sigma_o} = -\frac{t}{\lambda}$. The stress relaxation behavior is thus more accurately represented by a superposition of multiple relaxation processes governed by an array of time constants, λ_i. This, however, does not yet complete the entire story, as the measured macroscopic stress relaxation in essence reflects some sort of statistical average of processes involving stretched elastomeric blocks retracting, aggregates approaching one another, and blocks rejoining to establish the thermodynamically stable morphology. Hence, the morphological feature of the fluid evolves with time as stress relaxes. The stress relaxation time constants should therefore also vary with time. The deconvolution of the observed time-dependent stress into multiple time-variant relaxation processes is a difficult task at best, and will not be attempted here.

The rate of stress relaxation of both systems decreases gradually with time. Although the stress decays to levels difficult to detect at long times, the stress relaxation process also slows down to an imperceptible rate. Very small residual stress may indeed be trapped in the fluid. The question of why a sample sheared to a very long time (~1 hr.) was reported in literature to exhibit a much larger residual stress (3) than results of the present experiments awaits explanation. Apparently, subtle morphological variation persists even after the fluid has undergone shear for a considerable time and the stress ostensibly has reached a steady state.

Figure 10 shows the strain recovery data for both samples at three test temperatures. TR-41-1648 in general exhibits a higher total recovery than TR-41-1649. This observation is consistent with the large central PB block of TR-41-1648, sustaining much of the elastic deformation. The temperature dependence of recovery is opposite for the two block copolymers. Total

recovery increases with temperature for TR-41-1648, reflecting again the increased elastic deformation of the elastomeric PB block at high temperatures. In contrast, TR-16-1469 undergoes a more rapid and extensive recovery at lower temperatures. This may correspond to structural degradation to a lesser degree at low temperatures. Thus, the aggregates resulting from the flow-induced structure destruction are probably stronger at low temperatures, with numerous residual PB bridges connecting the PS fragments. This ultimately leads to faster and more complete strain recovery at low temperatures. At high temperatures, block pull-out proceeds to a greater extent, giving rise to small individual aggregates sustaining little elastic strain.

Acknowledgement

REFERENCES

[1]   M. Shen and H. Kawai, AIChE J., 24, 1 (1978).

[2]   J.A. Manson and L.H. Sperling, "Polymer Blends and Composites," Plenum, New York (1976).

[3]   A. Ghijsels and J. Raadsen, Pure Appl. Chem., 52, 1361 (1980).

[4]   G. Holden, E.T. Bishop, and L.R. Legge, J. Polym. Sci., C26, 37 (1969).

[5]   G. Kraus and J.T. Gruver, J. Appl. Polym. Sci., 11, 2121 (1967).

[6]   K.R. Arnold and D.J. Meier, J. Appl. Polym. Sci., 14, 427 (1970).

[7]   E.R. Pico and M.C. Williams, Nature, 259, 388 (1976).

[8]   C.I. Chung and J.C. Gale, J. Polym. Sci., Polym. Phys. Ed., 14, 1149 (1976).

[9]   P. Hanson, M.S. Thesis, University of California, Berkeley (1982).

[10] C.P. Henderson and M.C. Williams, J. Polym. Sci., Polymer Letters, 17, 257 (1979).

[11] E.V. Gouinlock and R.S. Porter, Polym. Eng. Sci., 17, 535 (1977).

[12] C.I. Chung, H.L. Griesbach, and L. Young, J. Polym. Sci., Polym. Sci., Polym. Phys. Ed., 18, 1237 (1980).

[13] D.F. Leary and M.C. Williams, J. Polym. Sci., Polym. Phys. Ed., 11, 345 (1973); ibid., 12, 265 (1974).

[14] S.L. Aggarwal, R.A. Livigni, L.F. Marka, and T.J. Dudek in "Block and Graft Copolymers," J.J. Burke and V. Weiss, ed., Syracuse University Press, N.Y. (1973).

[15] J.F. Beecher, L. Marker, R.D. Bradford, and S.L. Aggarwal, J. Polym. Sci., C26, 117 (1969).

[16] N.K. Kalfoglou, J. Appl. Polym. Sci., 23, 2673 (1979).

[17] E. Pedemonte, A. Turturro, and G. Dondero, Br. Polym. J., 6, 277 (1974).

[18] G. Akovali, J. Diamant, and M. Shen, J. Macromol. Sci., Phys. Ed., 13, 117 (1977).

[19] Y.D.M. Chen and R.E. Cohen, J. Appl. Polym. Sci., 21, 629 (1977).

[20] B. Maxwell and M. Nguyen, Polym. Eng. Sci., 19, 1140 (1979).

[21] J. Kelterborn and D.S. Soong, submitted to Polym. Eng. Sci.

[22] G. Kraus and R.W. Rollman, J. Polym. Sci., Polym. Phys. Ed., 14, 1133 (1976).

[23] J. Diamant, D.S. Soong and M.C. Williams in "Contemporary Topics in Polymer Science," vol. 4, W.J. Bailey and T. Tsuruta, ed., Plenum Press, New York, N.Y. (1982).

[24] T. Hashimoto, A. Todo, H. Itoi, and H. Kawai, Macromolecules, 10, 377 (1977).

[25] A. Todo, H. Uno, K. Miyoshi, T. Hashimoto, and H. Kawai, Polym. Eng. Sci., 17, 587 (1977).

[26] J.D. Ferry, "Viscoelastic Properties of Polymers," Wiley, New York (1980).

[27] M.L. Williams, R.F. Landel, and J.D. Ferry, J. Amer. Chem. Soc., 77, 3701 (1955).

[28] T.G. Fox and P.J. Flory, J. Appl. Phys., 21, 581 (1950).

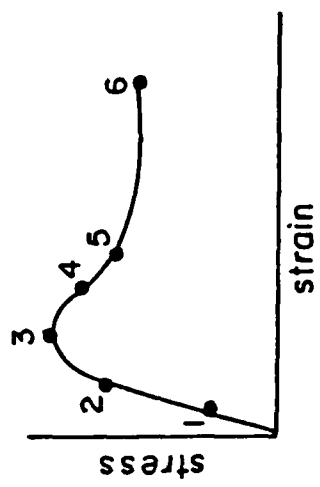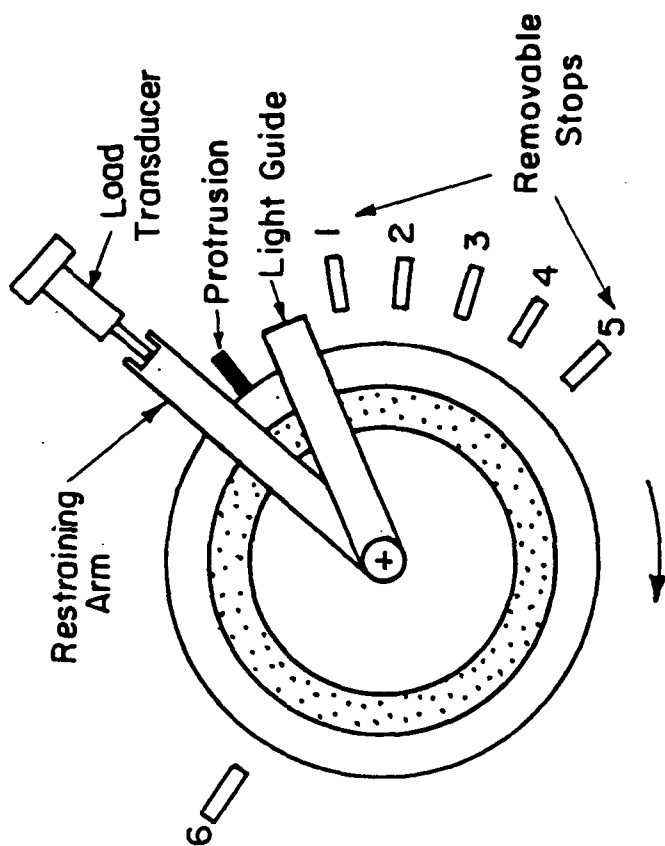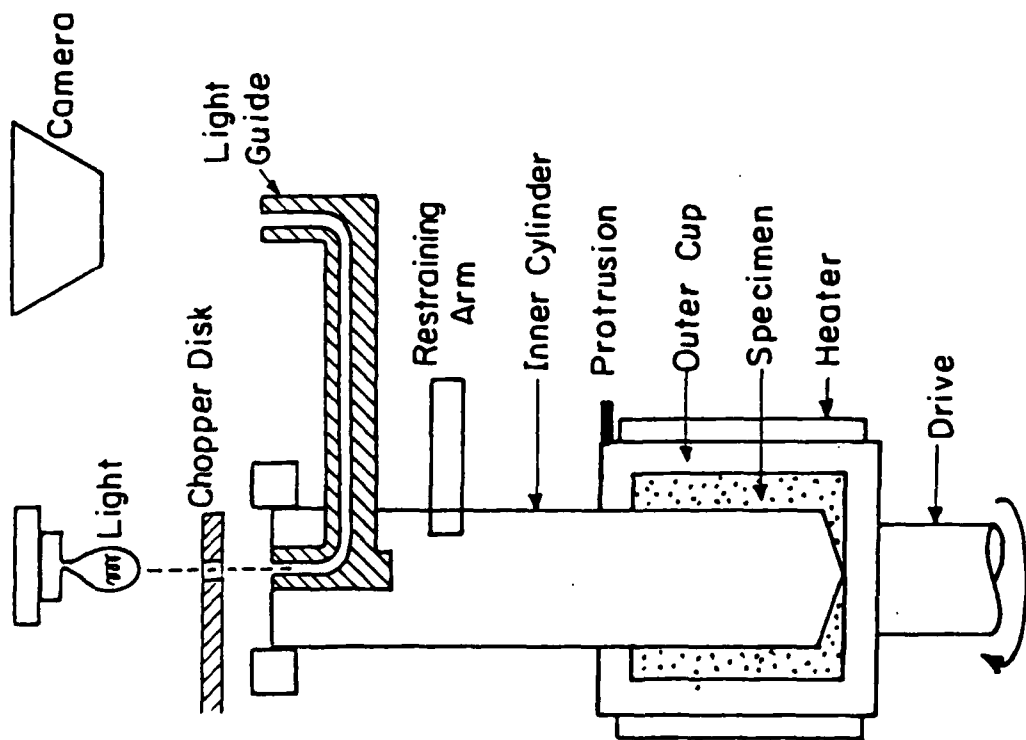TABLE 1. Composition and Molecular Specifications of the Test Samples

	TR-41-1649	TR-41-1648
	SBS (0.482 PS)	SBS (0.293 PS)
M_{S1}	14,000	16,000
M_B*	30,000	78,000
M_{S2}	14,000	16,000
total M	58,000	110,000

*Polybutadiene Microstructure

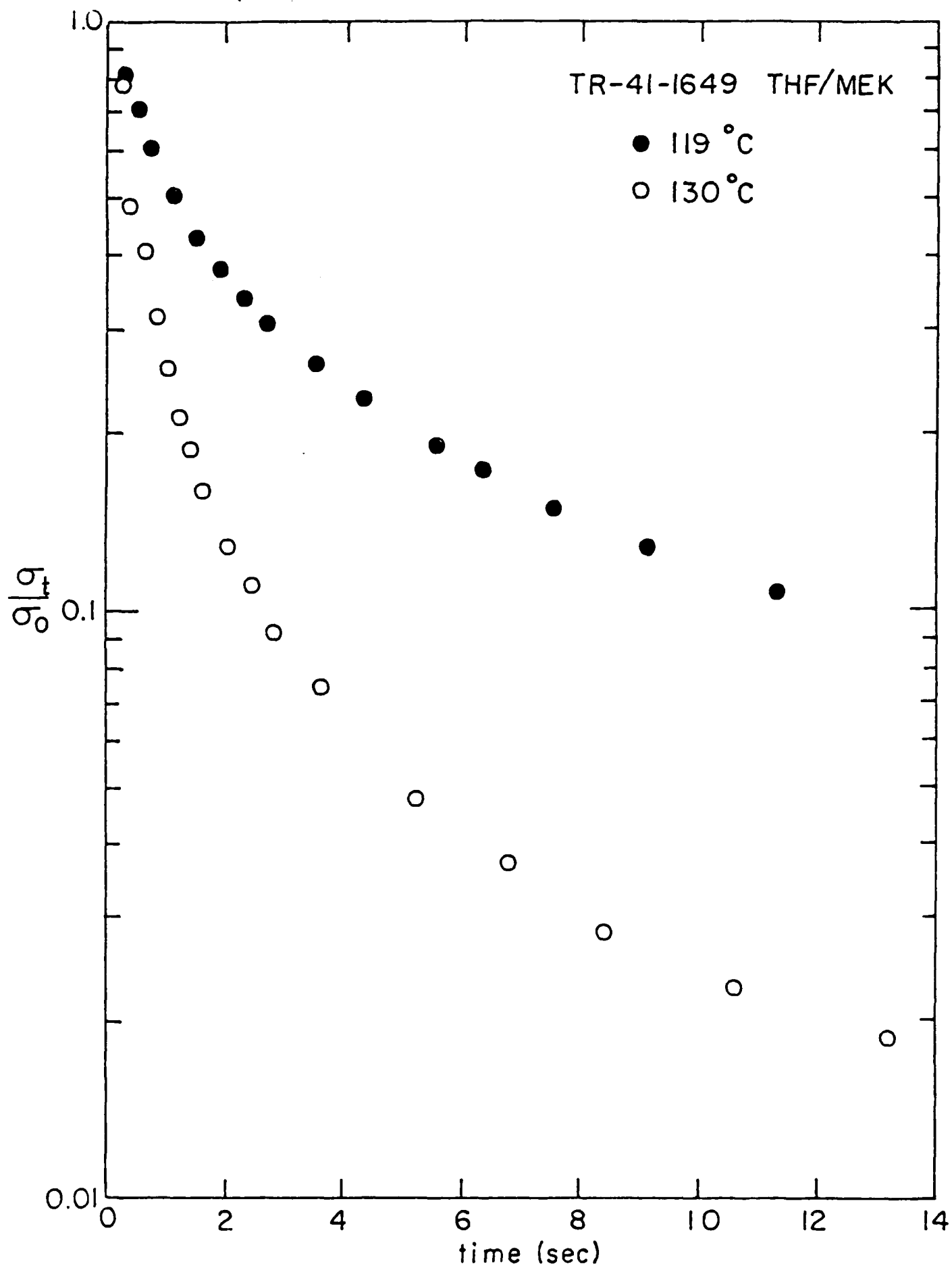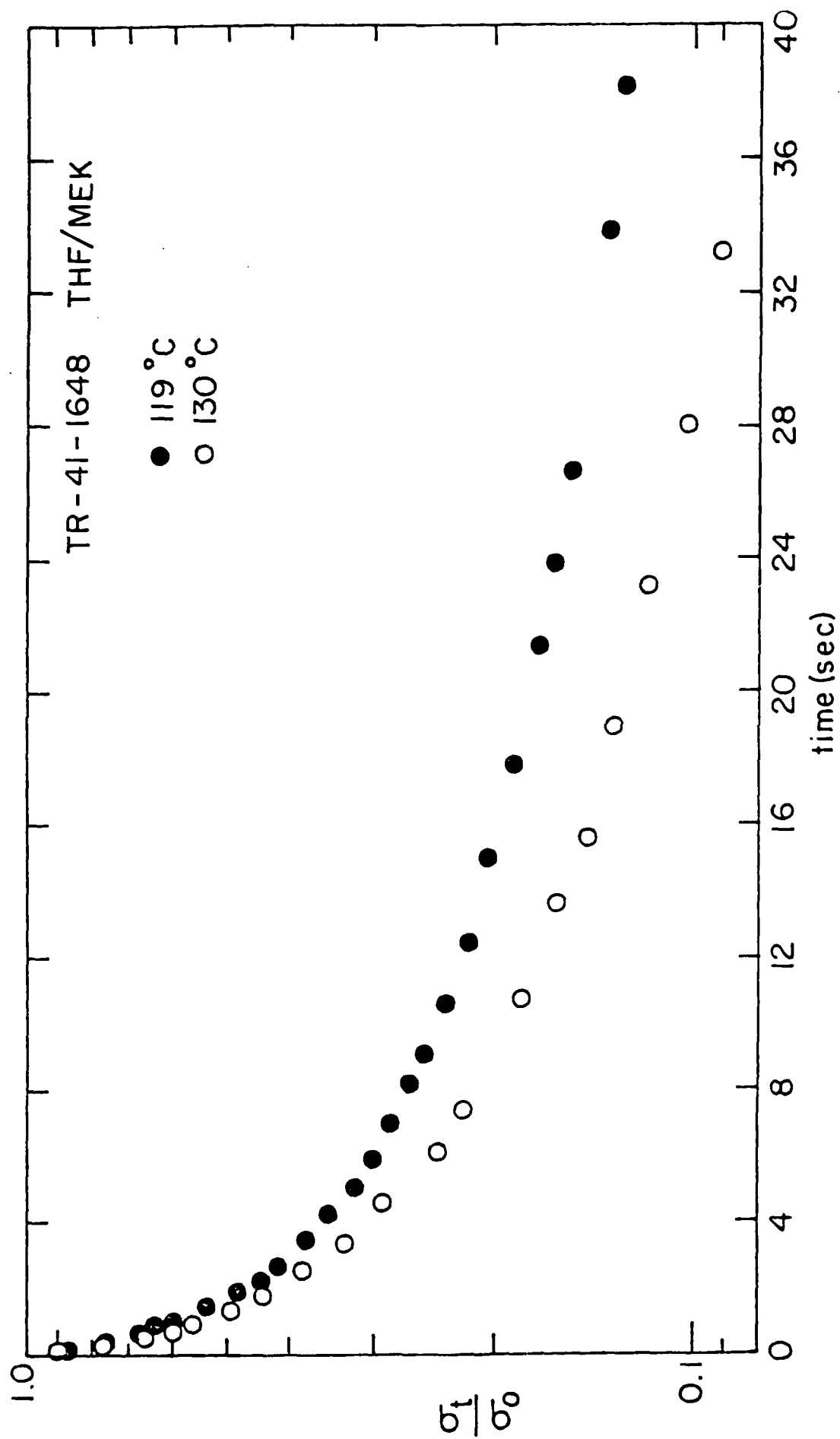|	
cis 1,4	40%
trans 1,4	50%
1,2	10%

FIGURE CAPTIONS

Fig. 1.   Diagrams of the Melt Elasticity Tester. The inset on the lower right-hand corner gives the approximate positions along the stress growth curve where the flow can be terminated by the removable stops.

Fig. 2.   Stress growth curves of TR-41-1649 at various test temperatures. The dashed curve corresponds to a sample that has been stored under 150°C for 7 hours.

Fig. 3.   Stress growth curves of TR-41-1648 at various test temperatures.

Fig. 4.   Normalized stress relaxation curves of TR-41-1649 cast from THF/MEK.

Fig. 5.   Normalized stress relaxation curves of TR-41-1648 cast from THF/MEK.

Fig. 6.   Effects of casting solvent on the stress relaxation behavior of TR-41-1649 at 119°C.

Fig. 7.   Effects of casting solvent on the stress relaxation behavior of TR-41-1648 at 119°C.

Fig. 8.   Stress relaxation following shear to various total strains for TR-41-1649.

Fig. 9.   Stress relaxation following shear to various total strains for TR-41-1648.

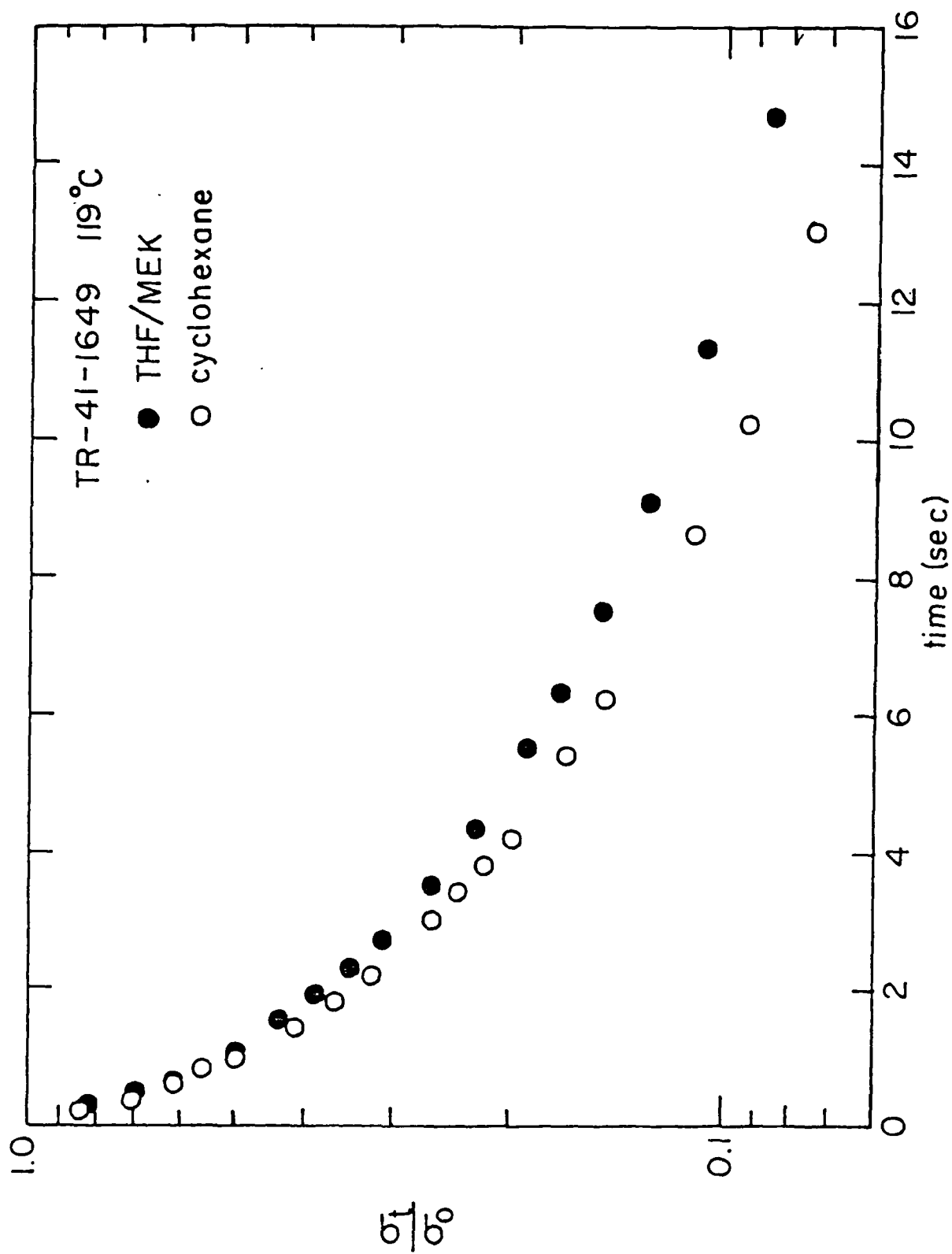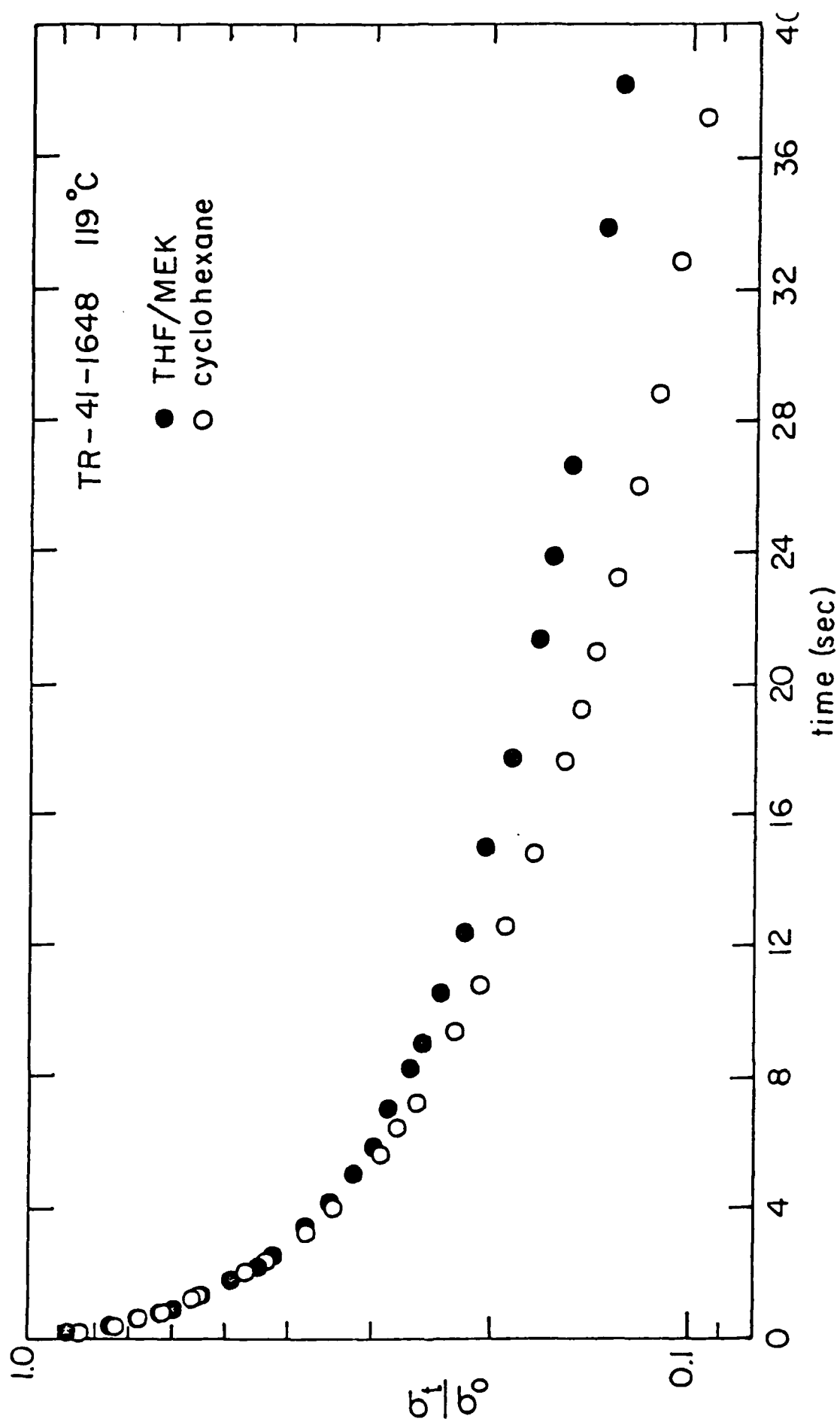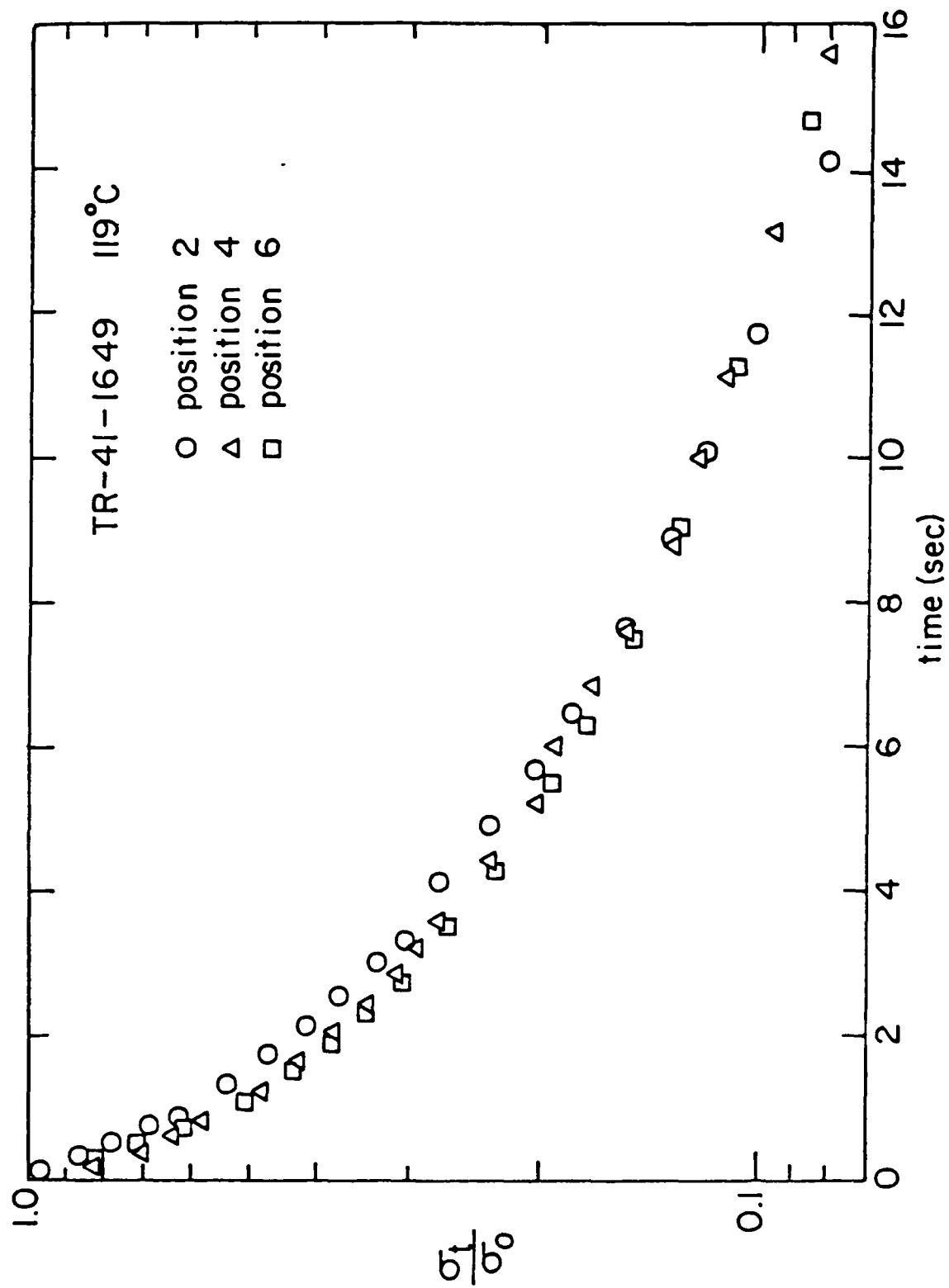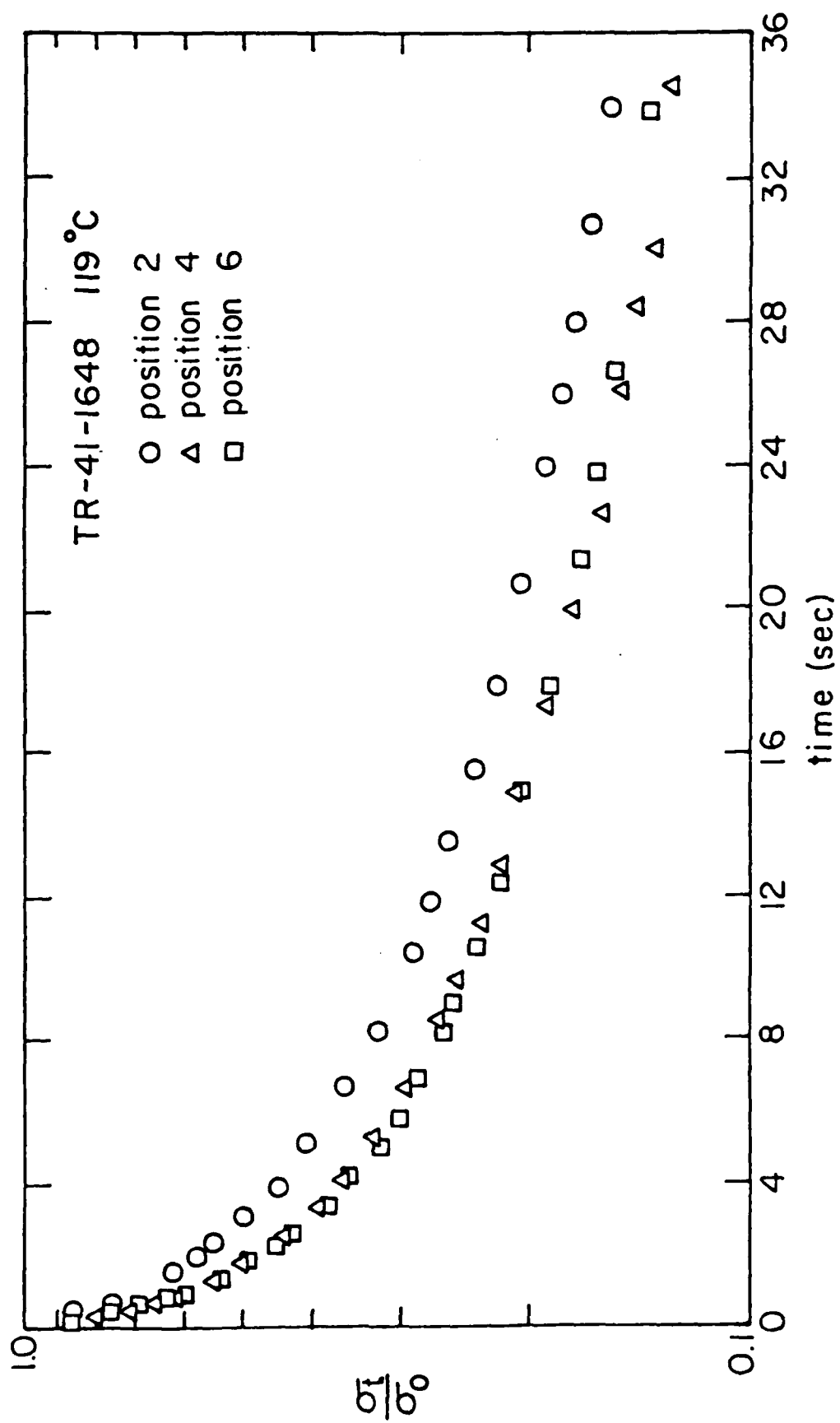Fig. 10.   Strain recovery curves for the two SBS samples at different temperatures.

Load
Transducer

Protrusion

Light Guide

Removable
Stops

Restraining
Arm

1

2

3

4

5

6

Camera

Light
Guide

Chopper Disk

Restraining
Arm

Inner Cylinder

Protrusion

Outer Cup

Specimen

Heater

Light

Drive

stress

strain

6

5

4

3

2

1

TR-41-1649

1. THF/MEK   119°C
2. cyclohexane 119°C
3. THF/MEK   130°C
4. THF/MEK   141°C
5. after 7 hrs at 150°C,
   run at 119°C

TR-41-1648

1. THF/MEK 119°C
2. cyclohexane 119°C
3. THF/MEK 130°C
4. THF/MEK 141°C

TR-41-1648   119°C

● THF/MEK
○ cyclohexane

TR-41-1649   119°C

O position 2
△ position 4
□ position 6

σ_t / σ_0

time (sec)

1.0

0.1

0   2   4   6   8   10   12   14   16

TR-41-1648 119°C

○ position 2
△ position 4
□ position 6

$\frac{\sigma}{\sigma_0}$

time (sec)

TR-41-1648
THF/MEK

119°C
130°C
141°C

TR-41-1649
THF/MEK

141°C
130°C
119°C

strain recoil

time (sec.)